JGR Solid Earth

RESEARCH ARTICLE
10.1029/2020JB020695

Heat-Blanketed Convection and its Implications for the Continental Lithosphere

K. Vilella[1,2] and F. Deschamps[1]

[1]Institute of Earth Sciences, Academia Sinica, TPE, Taiwan, [2]JSPS International Research Fellow, Hokkaido University, Sapporo, Hokkaido, Japan

Key Points:

- We study a mixed heated system where the internal heating is generated only within a horizontal layer close to the surface
- The convective system becomes insensitive to the presence of the heated layer when its thickness is extremely small
- When applied to Earth, our results suggest that the presence of continents does not impact significantly Earth's cooling rate

Supporting Information:

- Supporting Information S1

Correspondence to:
K. Vilella and F. Deschamps,
kennyvilella@gmail.com;
frederic@earth.sinica.edu.tw

Citation:
Vilella, K., & Deschamps, F. (2021). Heat-blanketed convection and its implications for the continental lithosphere. *Journal of Geophysical Research: Solid Earth*, *126*, e2020JB020695. https://doi.org/10.1029/2020JB020695

Received 30 JUL 2020
Accepted 22 DEC 2020

Abstract Earth's continental crust is characterized by a strong enrichment in long-lived radioactive isotopes. Recent estimates suggest that the continental crust contributes to 33% of the heat released at the surface of the Earth, while occupying less than 1% of the mantle. This distinctive feature has profound implications for the underlying mantle by impacting its thermal structure and heat transfer. However, the effects of a continental crust enriched in heat-producing elements on the underlying mantle have not yet been systematically investigated. Here, we conduct a preliminary investigation by considering a simplified convective system consisting in a mixed heated fluid where all the internal heating is concentrated in a top layer of thickness d_{HL} (referred to as "heat-blanketed convection"). We perform 24 numerical simulations in three dimensional Cartesian geometry for four specific set-ups and various values of d_{HL}. Our results suggest that the effects of the heated layer strongly depend on its thickness relative to the thickness of the thermal boundary layer (δ_{TBL}) in the homogeneous heating case ($d_{HL} = 1.0$). More specifically, for $d_{HL} > \delta_{TBL}$, the effects induced by the heated layer are quite modest, while, for $d_{HL} < \delta_{TBL}$, the properties of the convective system are strongly altered as d_{HL} decreases. In particular, the surface heat flux and convective vigor are significantly enhanced for very thin heated layers compared to the case $d_{HL} = 1.0$. The vertical distribution of heat producing elements may therefore play a key role in mantle dynamics. For Earth, the presence of continents should however not affect significantly the surface heat flux, and thus the Earth's cooling rate.

1. Introduction

Thermal evolution of Earth is mainly controlled by the convective transport of heat from its interior to its surface. This process is traditionally investigated using either numerical simulations of mantle dynamics (U. R. Christensen & Hofmann, 1994; Nakagawa & Tackley, 2004; Li et al., 2014) or analytical calculations of parametrized convection (Butler & Peltier, 2002; Grigné & Labrosse, 2001; Honda, 1995; Jellinek & Jackson, 2015; Sharpe & Peltier, 1978). A long-standing challenge for such models is their ability to incorporate self-consistently Earth's continents (Gurnis, 1988; Heron & Lowman, 2010, 2011; Jellinek & Jackson, 2015; Lenardic et al., 2005; Rolf & Tackley, 2011; Rolf et al., 2012; Tackley, 1998, 2000a, 2000b; Yoshida, 2013; Zhong & Gurnis, 1993, 1995), which are believed to affect the Earth's evolution substantially (Grigné & Labrosse, 2001; Korenaga, 2008). With the notable exception of Cooper et al. (2006), these studies have however neglected the enrichment of the continental crust in long-lived radioactive isotopes.

Recent estimates of the Earth's heat budget suggest that the heating rate in the continental crust is on average about 50 times higher than in the mantle (Jaupart et al., 2015). Such a large enrichment has important implications for the underlying mantle, as it impacts the heat flow and temperature at the base of the continental lithosphere (Jaupart et al., 1998). Mantle convection may in turn affect the conditions at the base of the continental lithosphere altering, for instance, their growth due to its thermal sensitivity (Jull & Kelemen, 2001).

Here, we perform a preliminary investigation addressing the effects of a heterogeneous source of internal heating on the convective system. In that aim, we conduct a series of 24 high resolution three dimensional numerical simulations of "heat-blanketed convection", a system where internal heating is generated only within a horizontal layer located close to the top surface. The thickness of the heated layer is systematically varied in order to quantify its effects on the properties of the system. In a last section, we discuss the potential implications of our results for the evolution and modeling of continents.

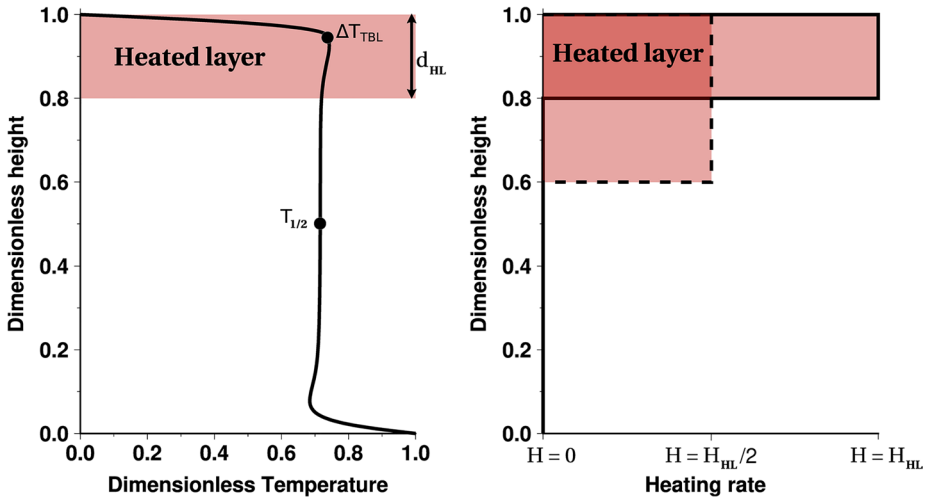

Figure 1. Schematic illustration of our physical model. Internal heating (right panel) is only included within a top "heat blanket" characterized by a thickness d_{HL} and a heating rate H_{HL} constant with time. The value of the heating rate H_{HL} changes with d_{HL} ($H_{HL} = H/d_{HL}$) in order to keep the same amount of generated heat (H). The influence of this layer will be inferred with the temperature profile (left panel) by measuring the temperature jump across the top thermal boundary layer (ΔT_{TBL}) and the temperature at mid-depth ($T_{1/2}$).

2. Model of Thermal Convection for a Heterogeneously Heated Fluid

2.1. Physical Model

Thermal convection driven by heterogeneous heating sources is derived from the homogeneous heating case, with which it shares many similarities. For the sake of clarity, we begin by presenting the more classical homogeneous heating case. This convective system is composed of a layer of volumetrically heated fluid encased between isothermal top and bottom surfaces. The top surface is colder than the bottom one such that the base may provide an additional source of heat (bottom heating). When assuming an isoviscous and incompressible fluid, the system is controlled by two dimensionless numbers, namely the Rayleigh number,

$$Ra = \frac{\rho g \alpha \Delta T d^3}{\kappa \eta}, \tag{1}$$

and the dimensionless heating rate,

$$H = \frac{h d^2}{\lambda \Delta T}, \tag{2}$$

where ρ is the density, g the gravitational acceleration, α the thermal expansion coefficient, ΔT the temperature jump across the fluid layer, d the layer thickness, η the dynamic viscosity, h the heating rate, λ the thermal conductivity and $\kappa = \lambda/\rho C_p$ the thermal diffusivity, with C_p the specific heat capacity at constant pressure. The Rayleigh number quantifies the vigor of convection with higher values of Ra implying stronger fluid motions and heat transfer. The dimensionless heating rate quantifies the relative importance of internal and bottom heating. With increasing heating rate, interior temperatures become hotter, which in turn reduces the heat flux from the core and weakens the power of upwelling plumes.

When considering heterogeneous heating, the convective system is identical to the one presented above except that internal heating is allowed to vary in time or/and space. Here, we seek to understand the fundamental mechanisms induced by heterogeneous heating that are valid independently of the distribution of internal heating. As a reference set-up, we therefore concentrate all the internal heating within a horizontal layer that remains stable with time and is located right below the surface, or "heat blanket" for short (Figure 1). The horizontal layer has a dimensionless thickness d_{HL}, which can be viewed as an additional controlling dimensionless number. Note that $d_{HL} = 1$ corresponds to the homogeneous case, while $d_{HL} = 0$ corresponds to a Rayleigh-Bénard system (without internal heating). We only consider few representative

thicknesses, and few representative values of the couple (Ra, H). This can be viewed as restrictive, but is necessary, since an exhaustive exploration of the space parameter would require an exaggerated computational time.

When changing the thickness of the heated layer at a given heating rate, one also changes the amount of generated heat. A different amount of heat is likely to cause important differences in the convective system. It is therefore more appropriate to compare numerical simulations with the same amount of heat involved. To do so, we modify the input value for the heating rate (H_{HL}) in our numerical simulations, such that the amount of generated heat remains constant when changing the thickness of the heat blanket ($H_{HL} = H/d_{HL}$). For the description of the model, we mention $H = H_{HL}d_{HL}$ corresponding to the equivalent heating rate in the homogeneous case.

2.2. Numerical Model

The numerical simulations of heat-blanketed convection are performed in three dimensional Cartesian geometry using the code StagYY (Tackley, 2008), which solves the dimensionless conservation equations of mass, momentum, and energy. Cartesian geometry may not be relevant for planetary mantles, but it allows to capture the effects of heterogeneous heating in a straightforward way. The top and bottom surfaces are isothermal and the mechanical boundary conditions are free slip, whereas the lateral boundary conditions are reflecting. All fluid properties are constant, except for density that depends on temperature in the buoyancy force (usually referred to as the Boussinesq, 1903, approximation). The initial temperature condition within the whole box is constant with a dimensionless value between 0.5 and 1.0. Note that the exact value is selected following the expected temperature of the well-mixed interior, in order to reduce computation time, while random, small amplitude (0.01 or 0.001), perturbations are superimposed in order to trigger convection. We stop the numerical simulation when a statistical steady state is reached. In practice, we determine the steady state as the stage for which both the volumetric average temperature and the surface heat flux are constant (their fluctuations are zero) when averaged over several overturn times.

For each couple (Ra, H) considered, we run one numerical simulation with a homogeneous heating rate ($d_{HL} = 1$) along with 4–8 additional simulations conducted for different values of d_{HL} (listed in Table 1). The selected aspect ratio and grid resolution (Table 1) guarantee both the development of a large number of convective currents (with a size that does not depend on the aspect ratio), and a good resolution in the thermal boundary layers (TBL) and convective currents (see Supplementary Material for more details). Moreover, this set of numerical simulations provides a good coverage for the possible values of the dimensionless numbers relevant to planetary bodies.

3. Heat-Blanketed Convection

The effects of the heat blanket on the convective system can be expressed by different processes, including changes in the temperature distribution and in the shape of convective currents. We therefore separate this exploration in three parts: (i) influence of the heat blanket thickness d_{HL} on the global characteristics of the convective system; (ii) variations in temperature profiles; and (iii) impacts on the flow pattern.

3.1. Global Characteristics

Characterizing thermal convection is challenging because the main properties of the system strongly vary both in space and time. A classical approach to overcome this issue is to focus on parameters that are spatially and/or temporally averaged. In particular, from a theoretical point of view, the convective system is often characterized using the horizontally and temporally averaged values of the surface heat flux (ϕ), temperature jump across the top thermal boundary layer (ΔT_{TBL}), and temperature at mid-depth ($T_{1/2}$), these properties providing a good description of the thermal state. In addition to the thermal state, it is useful to quantify the vigor of convection. For instance, the convective vigor can be quantified using the temporally and volume averaged root mean square velocity (V_{rms}). We also report the temporally and horizontally averaged surface velocity (V_h), which has the advantage to be easily measurable on Earth (e.g., Sella et al., 2002). These properties are reported in Table 1 for all the numerical simulations. Note that ΔT_{TBL} is here measured

Table 1
Input Parameters of the Numerical Simulations: The Rayleigh Number (Ra), the Dimensionless Heating Rate (H), the Thickness of the Heat Blanket (d_{HL}), See Text for More Details, the Grid Resolution in X:Y:Z Directions and the Domain Aspect Ratio in the X:Y:Z directions.

	d_{HL}	Resolution	Aspect	ϕ	Ur	ΔT_{TBL}	$T_{1/2}$	V_h	V_{rms}
	1	512 × 512 × 64	16:16:1	7.22 ± 0.00	0.831	1.282	1.156	39.1	31.2
	0.4	512 × 512 × 64	16:16:1	7.19 ± 0.03	0.834	1.175	0.982	24.9	19.8
$Ra = 10^4$	0.3	512 × 512 × 64	16:16:1	7.51 ± 0.00	0.799	1.057	0.913	27.2	21.9
$H = 6$	0.1	512 × 512 × 64	16:16:1	8.79 ± 0.00	0.683	0.947	0.639	50.0	38.5
	0.05	512 × 512 × 128	16:16:1	9.41 ± 0.00	0.638	0.956	0.565	55.0	42.1
	0.	1024 × 1024 × 64	32:32:1	4.37* ± 0.00	0.579	0.946	0.495	60.7	45.7
	1	768 × 768 × 128	12:12:1	12.43 ± 0.09	0.563	0.979	0.850	111	103
	0.4	768 × 768 × 128	12:12:1	12.06 ± 0.07	0.580	0.969	0.777	86.7	79.5
$Ra = 10^5$	0.3	768 × 768 × 128	12:12:1	12.04 ± 0.06	0.581	0.974	0.775	110	92.1
$H = 7$	0.1	768 × 768 × 128	12:12:1	13.21 ± 0.04	0.530	0.965	0.686	186	139
	0.05	768 × 768 × 128	12:12:1	14.13 ± 0.04	0.495	0.936	0.574	217	159
	0.	512 × 512 × 64	10:10:1	9.13* ± 0.04	0.434	0.933	0.495	236	173
	1	512 × 512 × 128	8:8:1	28.66 ± 0.26	0.698	1.023	0.912	338	276
	0.7	768 × 768 × 192	8:8:1	28.38 ± 0.19	0.705	1.029	0.871	268	214
	0.5	768 × 768 × 192	8:8:1	27.93 ± 0.18	0.716	1.031	0.802	219	185
	0.3	768 × 768 × 192	8:8:1	27.42 ± 0.13	0.729	1.037	0.748	171	178
$Ra = 10^6$	0.2	768 × 768 × 192	8:8:1	27.12 ± 0.12	0.737	1.034	0.733	159	195
$H = 20$	0.15	768 × 768 × 192	8:8:1	27.20 ± 0.11	0.735	1.051	0.751	178	208
	0.1	768 × 768 × 192	8:8:1	27.61 ± 0.19	0.724	0.989	0.799	330	295
	0.05	1536 × 1536 × 384	12:12:1	30.67 ± 0.11	0.652	0.977	0.707	662	505
	0.02	1536 × 1536 × 384	8:8:1	35.70 ± 0.10	0.560	0.932	0.613	774	604
	0.	1024 × 1024 × 512	6:6:1	19.72* ± 0.14	0.504	0.932	0.501	864	675
	1	768 × 768 × 192	8:8:1	57.95 ± 0.41	0.690	0.996	0.882	1233	902
	0.3	768 × 768 × 192	4:4:1	56.17 ± 0.32	0.712	0.971	0.721	541	608
$Ra = 10^7$	0.1	768 × 768 × 192	8:8:1	55.46 ± 0.18	0.721	0.983	0.691	514	811
$H = 40$	0.05	768 × 768 × 192	4:4:1	56.80 ± 0.47	0.704	1.015	0.788	1253	1208
	0.02	1024 × 1024 × 384	6:6:1	66.35 ± 0.44	0.603	0.967	0.690	2671	2138
	0.	1024 × 1024 × 512	8:8:1	41.45* ± 0.47	0.491	0.927	0.500	2722	2364

We also report some dimensionless characteristics of the system: ϕ the surface heat flux, $Ur = H/\phi$ the Urey ratio, ΔT_{TBL} the temperature jump across the top thermal boundary layer, $T_{1/2}$ the average temperature at mid-depth, V_h the average surface velocity, V_{rms} the volume average root mean square velocity.

* Note that the amount of internal heating H should be added to the heat flux for a meaningful comparison with other cases.

from the "hot" temperature profile composed of the hottest temperature at every depth (a discussion on the methods to define the thermal boundary layer is provided in the Supplementary Material). For the sake of simplicity, we will focus the description of the results only on the case conducted at $Ra = 10^6$ with $H = 20$, for which we have investigated a larger set of d_{HL} values. We have selected this specific case because the system is vigorous enough to exhibit a dynamics style similar to that of the Earth's mantle, although the spatial and temporal scales are different, while the required computational time remains reasonable.

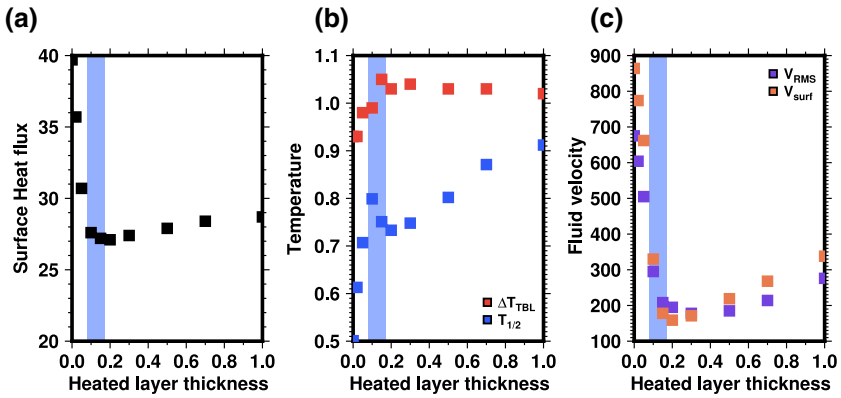

Figure 2. Variations of the dimensionless (a) surface heat flux, (b) temperature jump across the top thermal boundary layer (ΔT_{TBL}) and average temperature at mid-depth ($T_{1/2}$), (c) average surface velocity (V_h) and volume average root mean square velocity (V_{rms}) as a function of the dimensionless thickness of the heat blanket (d_{HL}). The numerical simulations are conducted for $Ra = 10^6$ and $H = 20$. The blue shaded area corresponds to the typical values for the thickness of the top thermal boundary layer (see Supplementary Material for more details) in the case where internal heating is homogeneous ($d_{\mathrm{HL}} = 1$). The case without internal heating ($d_{\mathrm{HL}} = 0$) is from Vilella and Deschamps (2018). Note that for this case the dimensionless surface heat flux is ~19.7. However, in order to achieve a meaningful comparison with cases including internal heating, we add to this number the amount of internal heating included in the other cases ($H = 20$).

Conclusions for this specific case are however fully consistent with results obtained for the three other cases (see Figure S3).

The results for the five properties investigated are plotted in Figure 2 as a function of d_{HL}. For $d_{\mathrm{HL}} = 0$, we report the results obtained by Vilella and Deschamps (2018) for pure bottom heating ($H = 0$). Figure 2 shows that the properties are changing continuously from values obtained without internal heating ($d_{\mathrm{HL}} = 0$) to values obtained for homogeneous heating ($d_{\mathrm{HL}} = 1$). This change is however not linear and is different for each property, so that a separate description is required. From $d_{\mathrm{HL}} = 1$ to 0.1, the surface heat flux is slightly decreasing (~3%) and then increases very sharply (~40%) until $d_{\mathrm{HL}} = 0$. Interestingly, we note that the transition between these two different behaviors occurs when the thickness of the heat blanket becomes smaller than the thickness of the top thermal boundary layer (δ_{TBL}) measured in the homogeneous case (blue shaded area). This observation is not surprising given that in internally heated systems the top thermal boundary layer controls the dynamics of the system. More specifically, when $d_{\mathrm{HL}} > \delta_{\mathrm{TBL}}$ the top thermal boundary layer is fully internally heated, which, following the theoretical framework of Vilella and Kaminski (2017), implies a direct relationship between the thermal structure of the top thermal boundary layer, the surface heat flux, and the Rayleigh number. Because the Rayleigh number is here constant, the surface heat flux and ΔT_{TBL} remain constant (Figure 2a and 2b), even if the interior temperature $T_{1/2}$ sharply decreases. The interior temperature $T_{1/2}$ is decreasing with d_{HL} simply because a decreasing portion of the convective interior is being heated. For $d_{\mathrm{HL}} < \delta_{\mathrm{TBL}}$, the top thermal boundary layer is no longer entirely heated so that it does not fully control the dynamics of the system. In particular, the thermal structure and heat transfer of the thermal boundary layer are now affected by hot plumes originating from the opposite thermal boundary layer. As for the surface heat flux, the temperature of the system is varying sharply until reaching the values obtained without internal heating. Surprisingly, ΔT_{TBL} and $T_{1/2}$ reach a peak when $d_{\mathrm{HL}} \approx \delta_{\mathrm{TBL}}$, a behavior that we discuss in section 3.2. Finally, the velocities V_h and V_{RMS}, characterizing the vigor of convection, are highly correlated with one another, and are further correlated to the surface heat flux. This is not surprising since a higher heat flux requires a more vigorous convection to transport the corresponding amount of heat. Interestingly, velocities are multiplied by a factor ~5 when d_{HL} decreases from 0.15 to 0, indicating that the enrichment of the internal heating in a thin layer strongly increases the convective vigor.

3.2. Temperature Profiles

Horizontally averaged temperature profiles for representative cases are plotted in Figure 3 (for other cases see Figure S4). As suggested in Figure 2b, the system is becoming colder as d_{HL} decreases (Figure 3a and 3b). We also observe that the thickness of the top thermal boundary layer is decreasing with decreasing d_{HL}. This can be easily explained by noting that the surface heat flux does not vary significantly, while a simple dimensional analysis indicates

$$\phi \sim k\frac{T_{1/2}}{\delta_{TBL}}, \tag{3}$$

implying that a lower $T_{1/2}$ should be balanced by a lower δ_{TBL}. For $d_{\mathrm{HL}} < \delta_{\mathrm{TBL}}$, the top thermal boundary layer is characterized by two trends with different temperature variations with depth (Figure 3a for $d_{\mathrm{HL}} = 0.1$ and $d_{\mathrm{HL}} = 0.05$). Within the heated layer, the thermal structure is equivalent to the one obtained for larger d_{HL}, while below the heat blanket, the thermal boundary layer tends to get closer to the thermal structure obtained in the case without internal heating. This behavior indicates that the thickness of the heated layer has to be extremely thin in order to have no effects on the thermal structure of the system. For $d_{\mathrm{HL}} > \delta_{\mathrm{TBL}}$, the thermal structure of the top thermal boundary layer only slightly changes with variations of d_{HL}. As a consequence, the temperature is clearly hotter within the heat blanket than below (Figure 3b for $d_{\mathrm{HL}} = 0.3$). For $d_{\mathrm{HL}} \approx \delta_{\mathrm{TBL}}$, we can see the formation of a peaked temperature at a depth corresponding to the base of the heated layer. As previously shown in Figure 2b, the interior temperature is slightly hotter in that case than for larger or lower values of d_{HL} (Figure 3b for $d_{\mathrm{HL}} = 0.05$ compared to $d_{\mathrm{HL}} = 0.02$ and 0.1).

In order to gain insight on the generation of instabilities, we have also plotted in Figure 3 the "hot" temperature profiles composed of the hottest temperature at every depth. This profile is particularly appropriate to assess the stability of the top thermal boundary layer (Vilella & Kaminski, 2017). Figure 3d shows that the "hot" temperature profile is also characterized by a peaked temperature, inducing a thicker, thus more stable, thermal boundary layer. As a consequence, the generation of cold instabilities should be more difficult, which in turn should reduce their ability to cool the convective interior. This may explain the increased interior temperature compared to cases with slightly larger or lower d_{HL} values. Another interesting result is that, for d_{HL} significantly lower than δ_{TBL} (Figure 3c for $d_{\mathrm{HL}} = 0.1$ and $d_{\mathrm{HL}} = 0.05$), the temperature profile does not change when d_{HL} is further reduced. We therefore expect that for cases with a very thin heated layer, further reducing d_{HL} does not alter the generation of cold downwellings (Figure 3c), but only modifies the thermal structure of the system (Figure 3a).

3.3. Planform of Convection

Previous observations have provided critical information on convective motions. For instance, the change of convective vigor may be deduced from the thickness of the heated layer. These inferences are however based on implicit arguments. In order to reach more robust conclusions, one may combine previous observations with the description of convection planforms reported in Figures 4–7. The systematic description of convection planforms has been conducted for Rayleigh-Bénard systems considering an isoviscous (Busse & Whitehead, 1971; Houseman, 1988; Parmentier & Sotin, 2000; Travis et al., 1990; Whitehead & Parsons, 1977) or strongly temperature dependent viscosity fluid (Christensen & Harder, 1991; White, 1988), and for purely internally heated systems (Houseman, 1988; Limare et al., 2015; Travis et al., 1990; Vilella et al., 2018). Such a study is however missing for mixed heating convection. By analogy with these extensive data sets, one can however draw general statements on the pattern obtained in this peculiar system.

In the homogeneous heating case ($d_{\mathrm{HL}} = 1.0$), the planforms are composed of focused cold downwellings with cylindrical shape at low *Ra* and more irregular elongated shape at larger *Ra* encased in an almost isothermal background. Hot upwellings are diffused and can be considered as a diffuse nonbuoyant return flow. These characteristics indicate the prevalence of internal heating over bottom heating. Furthermore, convection planforms reported for purely internally heated convection (Vilella et al., 2018) are qualitatively similar to the ones observed here. Interestingly, buoyant hot upwellings appear when d_{HL} is decreased suggesting that the importance of internal heating relative to bottom heating decreases, a trend supported

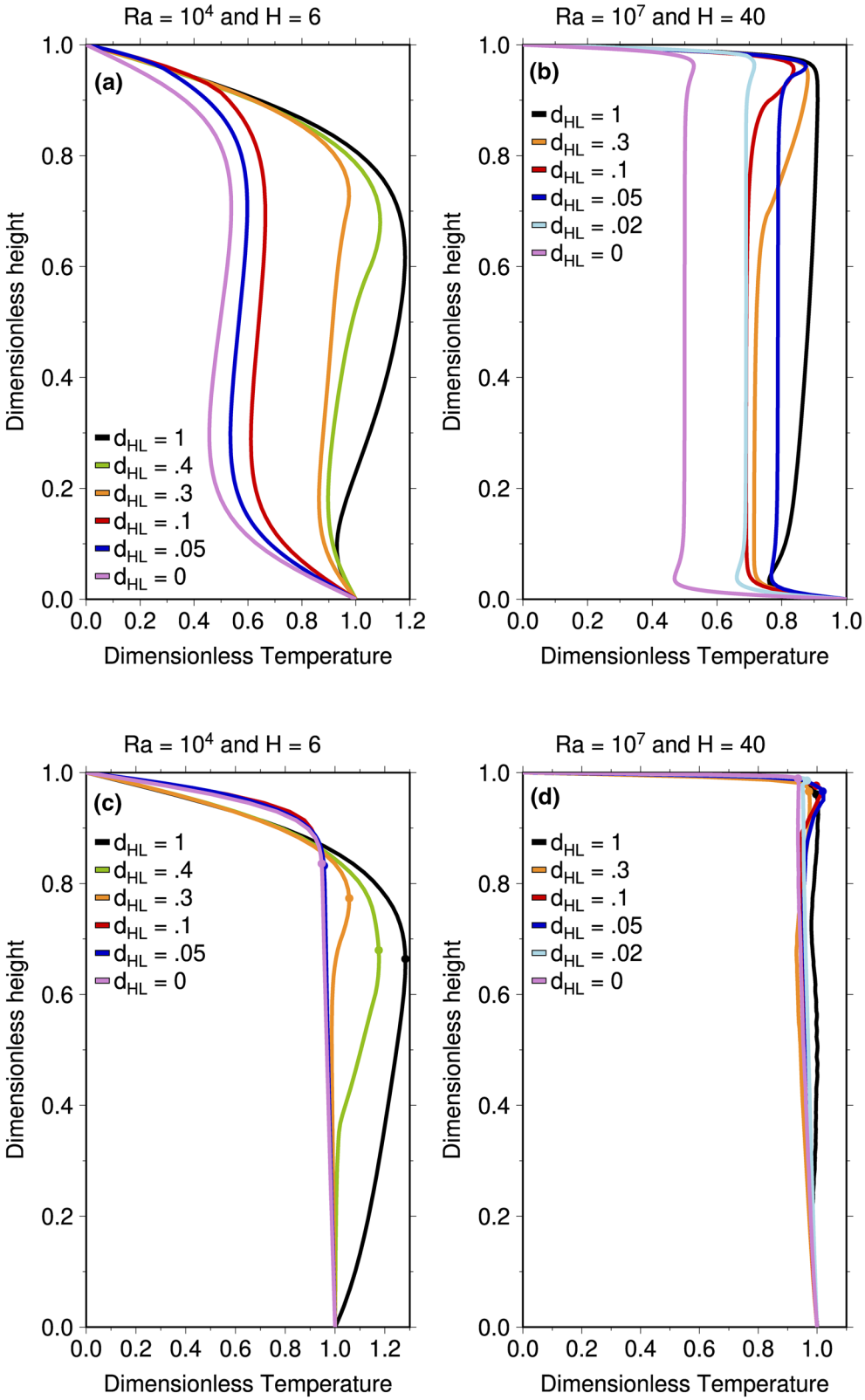

Figure 3. Horizontally averaged temperature profiles (top panels) and "hot" temperature profiles (bottom panels) for numerical simulations conducted with (a), (c) $Ra = 10^4$ with $H = 6$ and (b), (d) $Ra = 10^7$ with $H = 40$. "Hot" temperature profiles are built from the hottest temperature at a given depth. The base of the thermal boundary layer is indicated by a circle (see Supplementary Material for more details).

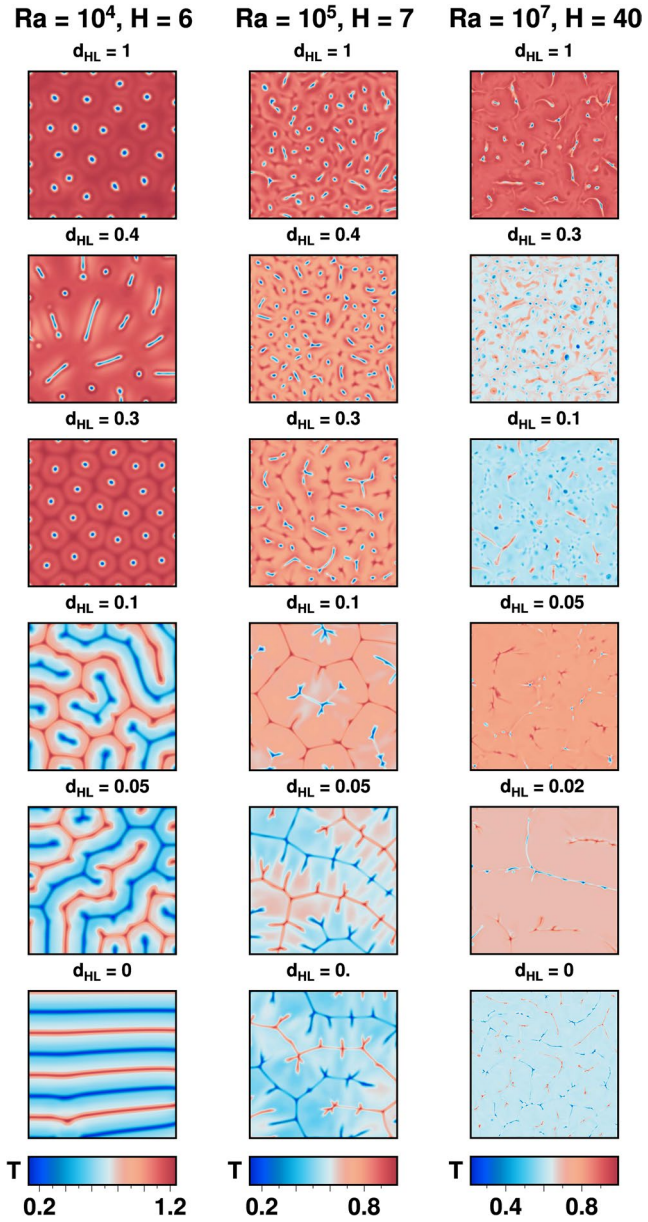

Figure 4. Convection planform at mid-depth for some cases described in Table 1. The color scale changes for each case in order to enhance the visibility of the convective structure. The domain aspect ratio of the planform represented is kept constant at a given Rayleigh number corresponding to the lower aspect ratio available (Table 1).

by the changes in Urey ratio as a function of d_{HL} (Table 1). Moreover, the strength and number of hot upwellings increase with decreasing d_{HL}. For $d_{HL} \ll \delta_{TBL}$, the convection planform even becomes similar to the case without internal heating ($d_{HL} = 0$) with cold downwellings and hot upwellings of equal strength and number. For such cases, ΔT_{TBL} does not change with varying d_{HL} (Figures 2 and S3) supporting our choice of using the "hot" temperature profile to assess the generation of cold downwellings by the top TBL. Furthermore, it is worth noting that, for $Ra = 10^7$, the case with the lowest d_{HL} is only slightly lower than δ_{TBL}. As a result, the planform of convection still exhibits some variations between the cases $d_{HL} = 0.02$ and $d_{HL} = 0$. This is unlikely caused by the higher Rayleigh number, but simply by the value of d_{HL}. For d_{HL} slightly lower than δ_{TBL} (for instance $Ra = 10^7$ and $d_{HL} = 0.02$), the hot upwellings and cold downwellings are forming sheet-like structures extending over a large spatial scale. The width of these convective structures are similar to the cases without internal heating, while the typical distance between two structures is increased. It may be possible that the thickness of the heat blanket introduces a new, thinner, spatial scale in the convective motions that strongly influences the pattern of convection.

4. Application to Earth's Continental Crust

Our numerical simulations have shown the potentially important effects of the vertical distribution of internal heating on the convective system. However, these effects highly depend on the relative thickness of the heated layer (d_{HL}) compared to the thickness of the thermal boundary layer (δ_{TBL}) in the homogeneous heating case ($d_{HL} = 1.0$). More precisely, for $d_{HL} > \delta_{TBL}$, only the interior temperature is affected by variations of d_{HL} (Figure 3). By contrast, for $d_{HL} < \delta_{TBL}$, all the properties of the convective system are changing importantly in response to potentially small changes of d_{HL}.

Interestingly, our model may be particularly appropriate to model Earth's continental crust, since this crust is characterized by a strong enrichment in heat producing elements. Indeed, the continental crust occupies less than 1% of the Earth's mantle while contributing to 33% of the heat produced by the decay of long-lived radioactive elements (Jaupart et al., 2007, 2015). The application of our numerical results requires first to identify the appropriate values for d_{HL} and δ_{TBL}. The estimate of d_{HL} is straightforward because it simply corresponds to the thickness of the continental crust. This thickness slightly varies across the globe with an average value of ~40 km and a maximum thickness of ~70 km (Mooney et al., 1998; Pasyanos et al., 2014). Taking a mantle thickness of 2,890 km, we obtain dimensionless thicknesses of $d_{HL} \approx 0.013$ on average and $d_{HL} \approx 0.024$ at a maximum so that the cases with $d_{HL} = 0.02$ may be appropriate to represent today's continental crust. Determining the thickness of the thermal boundary layer, or equivalently the Rayleigh number, of the mantle is more challenging. Different attempts to measure δ_{TBL} on Earth suggest a thickness of about 200 km (e.g., Lee et al., 2005). This corresponds to $\delta_{TBL} \approx 0.07$ and is compatible with values obtained for $Ra = 10^7$. In the past, it is likely that δ_{TBL} and d_{HL} were thinner, due to more vigorous convection, so that a larger Ra should be more appropriate for early Earth.

The application of our results to Earth's continental crust is however not straightforward. In particular, the models of convection presented here are clearly simplified compared to the Earth's mantle dynamics. It is therefore crucial to discuss the applicability of our models before applying our results to Earth's continental crust.

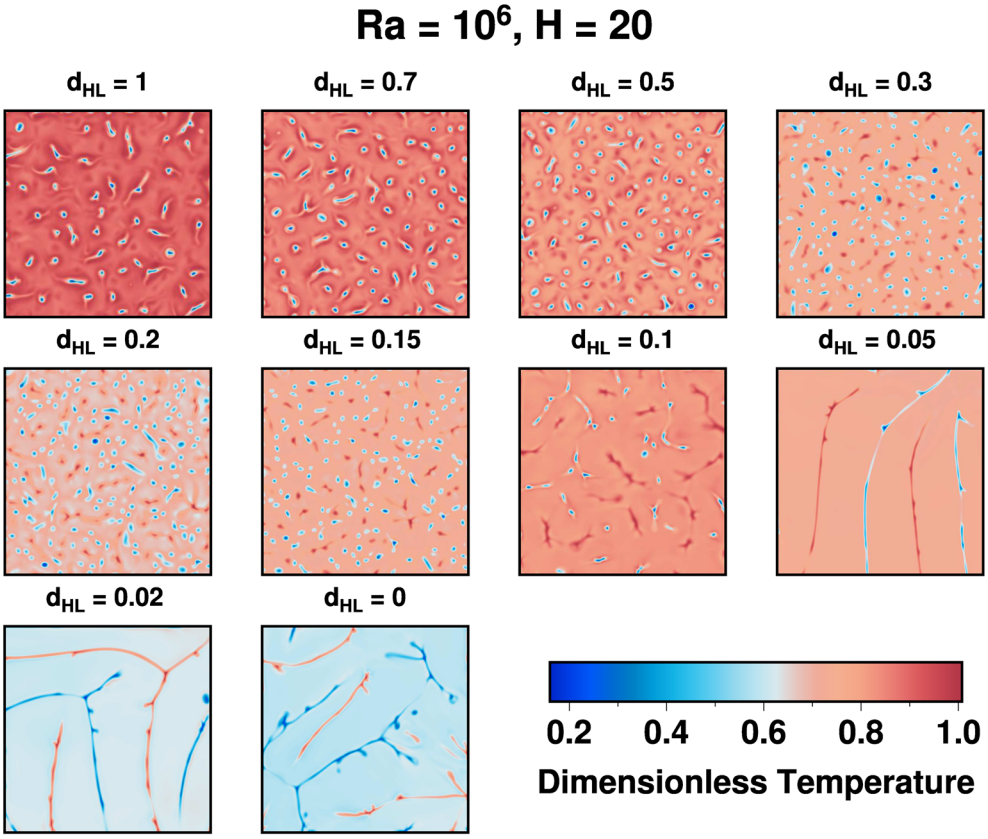

Figure 5. Convection planform at mid-depth for cases with $Ra = 10^6$ and $H = 20$ described in Table 1. The domain aspect ratio of the planform represented is kept constant to the lower aspect ratio available (Table 1).

4.1. Potential Applicability to Earth's Continental Crust

The purpose of this work is to identify the effects of a top layer enriched in heat-producing elements on the dynamics of the system. As such, many complexities of planetary mantles have been neglected or simplified in order to avoid any competitive effects. The advantage of this approach is to better understand the effects of different ingredients taken separately. The shortcoming, however, is the difficulty of predicting the effects of a single ingredient on the actual system, as the relative importance between different ingredients is difficult to assess. In other words, features not included in our model may potentially erase or even reverse some of our conclusions. It is therefore important to evaluate the potential impact of the main ingredients that are not included in our model.

A simplification of our model is to assume an isoviscous fluid rather than a complex rheology typical of mantle rocks. Rheology is a long-standing issue in models of planetary mantles. Traditionally, Newtonian rheologies with temperature and pressure dependent viscosity is considered for the bulk mantle, while rheology with plastic yielding have been used at the surface to mimic plate-like behavior (Moresi & Solomatov, 1998; Rolf & Tackley, 2011; Tackley, 2000a; Trompert & Hansen, 1998; Yoshida, 2013). The introduction of strongly temperature-dependent viscosity induces the formation of a stagnant lid at the top surface, where fluid motions are inhibited and conductive heat transport dominates. In addition, because heat is less easily extracted (Moresi & Solomatov, 1995, 1998), the interior temperature is larger than in the isoviscous case (Moresi & Solomatov, 1995). The flow pattern is dominated by plumes that are stopped beneath the stagnant lid. These properties are observed for both bottom-heated and mixed-heated systems (Stein et al., 2013). Note that the mobility of the lid decreases with increasing heating rate, that is the lid gets stiffer. The stagnant lid is often considered as an upward extension of the top TBL. In a planet whose mantle is animated by stagnant lid convection, we therefore expect that concentrating heat in a thin top layer would have effects similar to cases with $d_{HL} < \delta_{TBL}$. A strong and thick stagnant lid, however, is not observed on

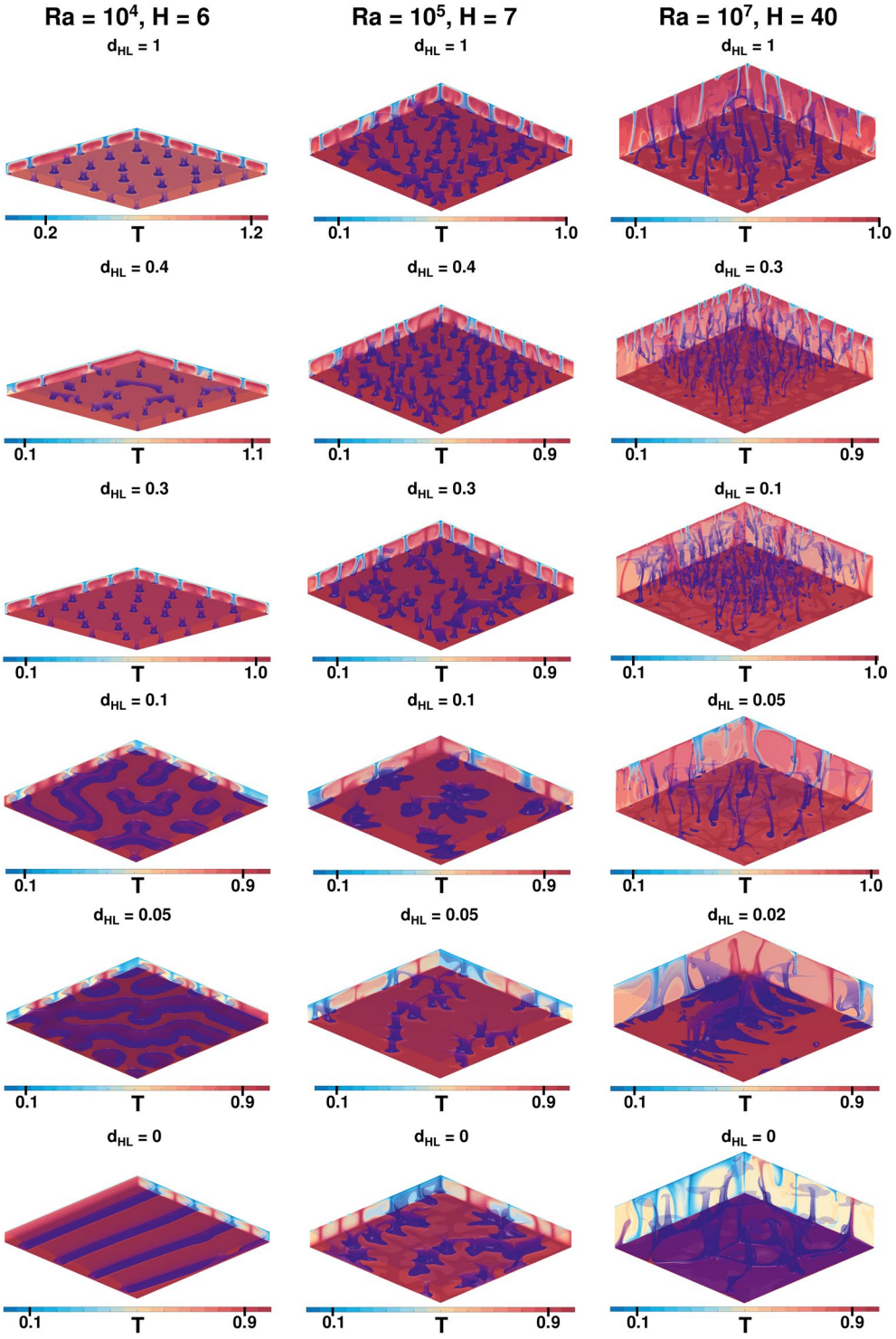

Figure 6. Isosurfaces of the cold downwellings for some cases described in Table 1. The color scale changes for each simulation in order to enhance the visibility of the convective structure. The domain aspect ratio of the temperature fields represented is kept constant at a given Rayleigh number corresponding to the lower aspect ratio available (Table 1).

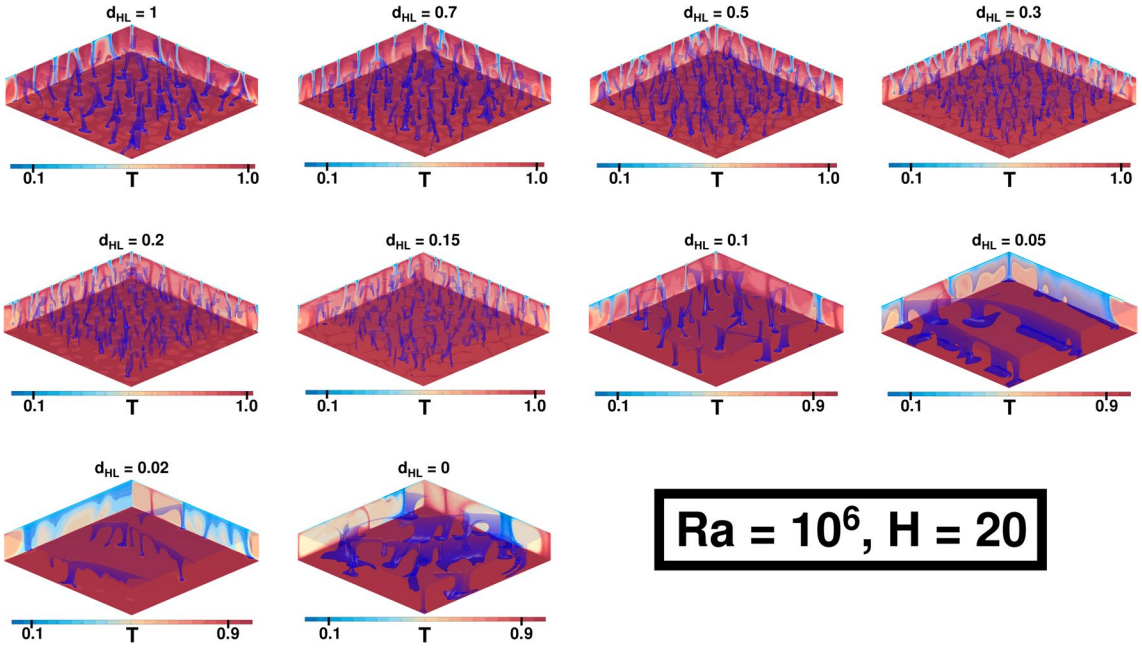

Figure 7. Isosurfaces of the cold downwellings for cases with $Ra = 10^6$ and $H = 20$ described in Table 1. The color scale changes for each simulation in order to enhance the visibility of the convective structure. The domain aspect ratio of the temperature fields represented is kept constant to the lower aspect ratio available (Table 1).

Earth. Plastic yielding is therefore introduced as a weakening mechanism to allow for the break-up of this lid, leading to a so-called mobile-lid regime. While a stagnant lid is not present, the interior temperature and heat flux remain larger and lower, respectively, than in the isoviscous case (as suggested by recent global models Deschamps et al., 2018; Deschamps & Li, 2019, see Supplementary Material and Table S2), leading to thicker TBLs. Overall, the introduction of a more realistic rheology should impact importantly the convection planform (White, 1988), while increasing the interior temperature and thickness of the top TBL, such that the case $d_{HL} < \delta_{TBL}$ would be reached more easily.

A second important difference between our model and Earth's continental crust is that our heat-blanket covers the whole system, while Earth's continents cover only 30%–40% of Earth's surface (Taylor & McLennan, 1995). The effects of continent coverage on the convective system have been investigated with both numerical simulations (Coltice et al., 2014; Cooper et al., 2006; Jellinek & Lenardic, 2009; Lenardic et al., 2005; Whitehead & Behn, 2015) and laboratory experiments (Guillou & Jaupart, 1995; Jellinek & Lenardic, 2009; Lenardic et al., 2005). A major finding is the existence of two different regimes depending on the continent coverage (Lenardic et al., 2005). For a surface area covered by continents lower than about 40%, the heat flux remains high with plate-like motions at the top surface, whereas, for a larger continent coverage, a stagnant lid appears at the top, reducing significantly the surface heat flux. Note, however, that this transition occurs at greater continent coverage with decreasing Rayleigh number and even disappears for low *Ra*. When applied to Earth, one may expect a very moderate effect of continent coverage on the surface heat flux, as Earth should remain throughout its evolution in the high heat flux regime. Nevertheless, partial coverage of continents should still impact mantle dynamics by inducing a large scale motion in the system (Guillou & Jaupart, 1995) and by increasing the production rate of sea floor (Coltice et al., 2014). Moreover, continental drift may affect the convective motions in the mantle by focusing cold downwellings on the edge of continents and disrupting the convective cells (Whitehead & Behn, 2015).

It is also important to note that the heat blanket in our numerical model is a part of the convective system, while the low amount of material exchange between continents and the mantle suggests that continents remain mostly separated from the mantle. Nevertheless, abundant evidence, such as the small heat flux inferred below continents compared to the estimated heat flux below the oceanic lithosphere (Jaupart & Mareschal, 2011; Jaupart et al., 2016; McKenzie & Bickle, 1988; Putirka et al., 2007), show that continents

have an impact on the thermal structure of the mantle and thus its dynamics. As such, the incorporation of the heat blanket within the convective system may be a reasonable assumption.

A last difference between our numerical models and Earth is the presence of internal heating not only in the enriched layer but also in the bulk system. To overcome this issue, one may consider an idealized version of Earth's evolution. At first, the mantle should be characterized with a homogeneous distribution of internal heating, while the subsequent evolution and chemical differentiation should induce the creation and thickening of a top layer enriched in heat producing elements. At one point, the enriched layer reaches a critical thickness $d_{HL,cr}$ for which all the long-lived radioactive elements have been extracted from the mantle. For Earth, $d_{HL,cr}$ should be around 0.06, at first order. This evolution is obviously figurative as the initial Earth's mantle is likely to be highly heterogeneous, while, in practice, it seems difficult to extract all the long-lived radioactive elements from the mantle. However, although idealized, this evolution is interesting because the initial and final stages can be represented by our numerical models. We may therefore use these two end-member cases to somewhat constrain the overall effect of the continental crust on the convective system. More specifically, considering the representative case $Ra = 10^7$, we can compare the results from the initial stage ($d_{HL} = 1.0$) and final stage ($d_{HL} = 0.06$, which can be approximated by our case at $d_{HL} = 0.05$) using results reported in Table 1 and Figure S3. These results indicate that, except for the interior temperature, properties are only slightly impacted by the presence of the heated layer. In particular, the surface heat flux should not be impacted by the presence of the heated layer, which is likely to be valid for more complex systems, as shown by results of Cooper et al. (2006).

4.2. Are Continents Preventing Earth Cooling?

It has been suggested that the heat produced by the radioactive isotopes in the continental crust does not participate in convection, and therefore should not be included in the long-term evolution of the Earth's mantle. An interesting by-product of this hypothesis is that enriching the continental crust in long-lived radioactive isotopes allows removing heat from the Earth's mantle, which in turn induces a lower cooling rate (Grigné & Labrosse, 2001). This has been used, for instance, to explain the thermal evolution of Earth (e.g., Jellinek & Jackson, 2015).

An evidence supporting this scenario is the low heat flux beneath the continental lithosphere compared to that beneath the oceanic lithosphere (≈65 mW m^{-2} and ≈100 mW m^{-2}, respectively, following Jaupart & Mareschal, 2011; Jaupart et al., 2016, and reference therein). However, the differences between the oceanic and continental lithospheres are such that a direct comparison between these two regions may not be relevant. For instance, a specificity of the oceanic lithosphere is that heat is dominantly transported by volcanism (Jaupart et al., 2015), which stands as a much more efficient way to transport heat. Overall, our results suggest that the continental crust is thick enough to affect significantly mantle dynamics. It is therefore inappropriate to consider the heat produced in the continental crust as separated from the mantle. As discussed in section 4.1, and in agreement with Cooper et al. (2006), the surface heat flux, and thus the cooling rate, should not be significantly affected by the partitioning of heat in the heated layer.

It is important to note that our results are valid as long as solid-state thermal convection and thermal conduction are the dominant heat transfer processes. In particular, volcanism is another mode of heat transfer that is not considered in our models and that should change importantly the conclusions we draw. This, when applying to the Earth's case, explains why our results should not be applied to the oceanic lithosphere, while they may be relevant for describing the continental crust, where volcanism is not an important mode of heat transport.

4.3. Control on the Thickness of the Continental Crust

Observations have shown that the continental crust is characterized by a very homogeneous thickness of 35–45 km (Mooney et al., 1998; Pasyanos et al., 2014). At first glance, this homogeneity seems inconsistent with the complexity of Earth's dynamics and the large compositional heterogeneities of the Earth's mantle. To overcome this issue, the presence of some mechanisms controlling the thickness of the continental crust is traditionally invoked. In particular, it has been proposed that the pressure and temperature conditions play a key role in the production of the continental crust (Jull & Kelemen, 2001). Below a certain depth, the

conditions are no longer suitable for the production of continental crust, which sets an upper limit for the thickness of the continental crust. Considering the simplifications of our model, it is not possible to draw clear and safe conclusions on the potential effects of the heated layer on the thickness of Earth's continental crust.

Alternatively, an interesting exercise is to study a different rocky planet, for instance a Mars-like planet. In that case, due to the lower gravitational acceleration, the limiting depth for the production of crust may be significantly deeper. Interestingly, following the exact crustal thickness, it is possible to reach the regime where $\delta_{TBL} \approx d_{HL}$. Assuming that the increase of temperature reported in that regime (Figure 2) is still present in a more realistic system, one may expect an increase in the crustal production rate. After this episode of enhanced crustal production, the temperature should decrease while the thickness of the thermal boundary layer should increase (Figure 3c and 3d), both effects making the generation of volcanism more difficult. It is therefore possible that on Mars-like planet the crustal thickness is bound to be slightly larger than δ_{TBL}. This specific condition may be characterized by a slightly lower surface heat flux (Figure 2a) as well as a more sluggish convection (Figure 2c), which is compatible with our understanding of Mars dynamics.

4.4. Are Continents Acting as Insulators?

It is generally thought that continents act as thermal insulators, reducing the surface heat flux. This idea originates from the small heat flux inferred below continents compared to below the oceanic lithosphere (McKenzie & Bickle, 1988; Jaupart & Mareschal, 2011; Jaupart et al., 2016; Putirka et al., 2007). This observation has led some authors to model continents by prescribing an insulator layer at the top surface (Heron & Lowman, 2010, 2011). Alternatively, other authors prescribed a large viscosity jump within continents (Cooper et al., 2013; Gurnis, 1988; Lenardic et al., 2011, 2005; Rolf & Tackley, 2011; Rolf et al., 2012; Zhong & Gurnis, 1993) inducing a thicker thermal boundary layer, in agreement with the higher thickness of the continental lithosphere compared to the oceanic lithosphere, which in turn causes an insulation effect. These models, however, do not include the enrichment in heat producing elements within the continental crust.

Our results suggest that enriching a superficial layer in radioactive isotopes should induce a modest variation of the surface heat flux, which may be viewed as inconsistent with observations. In that case, however, the surface heat flux does not necessarily reflect the heat flux below the heated layer, since a large amount of heat is produced within the heated layer. Actually, the heat flux below the heat blanket seems to be minimum when $d_{HL} \approx \delta_{TBL}$, while remaining low for cases appropriate for the Earth's mantle. Therefore, it appears that the enrichment of the continental crust in radioactive isotopes may be partly responsible for the small heat flux inferred below continents.

5. Conclusion

We have investigated the effects of heterogeneous internal heating by studying a convective system where internal heating is only present in a top horizontal layer. Different behaviors have been observed following the thickness of the heat blanket (d_{HL}) compared to the thickness of the thermal boundary layer in the homogeneous case (δ_{TBL}). For a "thick" heat blanket ($d_{HL} > \delta_{TBL}$), the convective system is generally equivalent to the system with homogeneous heating ($d_{HL} = 1.0$). The only noteworthy effect is a decrease of the interior temperature with decreasing value of d_{HL} (Figures 2b and 3a,b). The case $d_{HL} \approx \delta_{TBL}$ marks a transition between two different regimes. A peculiarity of this case is the peaked temperature observed in both the horizontally averaged and "hot" temperature profiles (Figures 2b and 3). We interpret this feature as the result of a weakening of the generation of cold downwellings, which in turn reduces their ability to cool down the system. For $d_{HL} < \delta_{TBL}$, all the system properties change quickly with decreasing value of d_{HL} until it becomes equal to those obtained for the case without any internal heating ($d_{HL} = 0$). In particular, the surface heat flux (Figure 2a) and convective vigor (Figure 2c) strongly increase with decreasing d_{HL}. This can be explained by the appearance and strengthening of hot upwellings (Figures 4 and 5). At the same time, the system is cooling down and tends to reach the thermal structure of the system without internal heating (Figures 2b and 3). For $d_{HL} \ll \delta_{TBL}$, the convection planform does not change significantly as d_{HL} decreases (Figures 4 and 5), while the surface heat flux and convective vigor are still modified substantially with decreasing d_{HL}.

Our results therefore suggest that there is a continuous change from the homogeneous heating case to the case without internal heating. Nevertheless, an extremely thin heated layer is required to totally suppress the effect of the heated layer on the properties of the convective system. As a consequence, the crustal enrichment in radioactive isotopes is a major feature of planetary bodies that should not be neglected. For instance, the low surface heat flux observed beneath continents may be at least partly the result of such an enrichment. Moreover, the small variations of the surface heat flux induced by the presence of the heat blanket support a minor impact of the presence of continents on the cooling rate of Earth. By contrast, we speculate that in smaller rocky planets the cooling rate and the convective vigor may be reduced by the presence of an enriched crust, provided that the crustal thickness is slightly larger than δ_{TBL}. From a more general point of view, our results indicate the existence of different regimes characterized by very different properties depending on the crustal thickness. These regimes may induce a certain variability of dynamics style on rocky planets. The vertical distribution of heat producing elements would then be a key ingredient to understand the thermal state and evolution of a planet.

Data Availability Statement

The data used for generating the figures are available for academic purposes (Vilella, 2020). The code used in this work is not publicly available but was thoroughly described in Tackley (2008).

Acknowledgments
The authors are grateful to Tobias Rolf and Alana Semple for their careful and constructive reviews that helped us to greatly improve this manuscript. This research was funded by the Ministry of Science and Technology of Taiwan (MOST) Grants 106-2116-M-001-014 and 107-2116-M-001-010 and by JSPS KAKENHI Grant JP19F19023. Numerical computations were performed on IESAS Linux Cluster and on the cluster of Hokkaido University. The interpretation of the results benefited from discussions with Claude Jaupart.

References

Boussinesq, J. (1903). *Théorie analytique de la chaleur mise en harmonie avec la thermodynamique et avec la théorie mécanique de la lumière, Tome II*. Paris: Gauthier-Villars. (pp. A67–A68).
Busse, F. H., & Whitehead, J. A. (1971). Instabilities of convection rolls in a high Prandtl number fluid. *Journal of Fluid Mechanics*, *47*, 305–320. https://doi.org/10.1017/S002211207900015X
Butler, S. L., & Peltier, W. R. (2002). Thermal evolution of Earth: Models with time-dependent layering of mantle convection which satisfy the Urey ratio constraint. *Journal of Geophysical Research*, *107*, ESE3-1–ESE3-15. https://doi.org/10.1029/2000JB000018
Christensen, U., & Harder, H. (1991). 3-D Convection with variable viscosity. *Geophysical Journal International*, *104*, 213–226. https://doi.org/10.1111/j.1365-246X.1991.tb02505.x
Christensen, U. R., & Hofmann, A. W. (1994). Segregation of subducted oceanic crust in the convecting mantle. *Journal of Geophysical Research*, *99*, 19867–19884. https://doi.org/10.1029/93JB03403
Coltice, N., Rolf, T., & Tackley, P. J. (2014). Seafloor spreading evolution in response to continental growth. *Geology*, *42*, 235–238. https://doi.org/10.1130/G35062.1
Cooper, C. M., Lenardic, A., & Moresi, L. N. (2006). Effects of continental insulation and the partitioning of heat producing elements on the Earth's heat loss. *Geophysical Research Letters*, *33*, L13313. https://doi.org/10.1029/2006GL026291
Cooper, C. M., Moresi, L. N., & Lenardic, A. (2013). Effects of continental configuration on mantle heat loss. *Geophysical Research Letters*, *40*, 2647–2651. https://doi.org/10.1002/grl.50547
Deschamps, F., & Li, Y. (2019). Core-Mantle boundary dynamic topography: Influence of Postperovskite viscosity. *Journal of Geophysical Research: Solid Earth*, *124*, 9247–9264. https://doi.org/10.1029/2019JB017859
Deschamps, F., Rogister, Y., & Tackley, P. J. (2018). Constraints on core-mantle boundary topography from models of thermal and thermo-chemical convection. *Geophysical Journal International*, *212*, 164–188. https://doi.org/10.1093/gji/ggx402
Grigné, C., & Labrosse, S. (2001). Effects of continents on Earth cooling: Thermal blanketing and depletion in radioactive elements. *Geophysical Research Letters*, *28*, 2707–2710. https://doi.org/10.1029/2000GL012475
Guillou, L., & Jaupart, C. (1995). On the effect of continents on mantle convection. *Journal of Geophysical Research*, *100*(B12), 24217–24238.
Gurnis, M. (1988). Large-scale mantle convection and the aggregation and dispersal of supercontinents. *Nature*, *332*(6166), 695–699.
Heron, P. J., & Lowman, J. P. (2010). Thermal response of the mantle following the formation of a "super-plate". *Geophysical Research Letters*, *37*, L22302. https://doi.org/10.1029/2010GL045136
Heron, P. J., & Lowman, J. P. (2011). The effects of supercontinent size and thermal insulation on the formation of mantle plumes. *Tectonophysics*, *510*, 28–38. https://doi.org/10.1016/j.tecto.2011.07.002
Honda, S. (1995). A simple parameterized model of Earth's thermal history with the transition from layered to whole mantle convection. *Earth and Planetary Science Letters*, *131*, 357–369. https://doi.org/10.1016/0012-821X(95)00034-A
Houseman, G. (1988). The dependence of convection planform on mode of heating. *Nature*, *332*, 346–349. https://doi.org/10.1038/332346a0
Jaupart, C., Labrosse, S., Lucazeau, F., & Mareschal, J. C. (2015). *Temperatures, heat and energy in the mantle of the Earth*. https://doi.org/10.1016/B978-0-444-53802-4.00126-3
Jaupart, C., Labrosse, S., & Mareschal, J. C. (2007). Temperatures, heat and energy in the mantle of the Earth. In D. Bercovici & G. Schubert (Eds.), *Mantle dynamics*. (Vol. 7, pp. 253–303). Elsevier. https://doi.org/10.1016/B978-044452748-6.00114-0
Jaupart, C., & Mareschal, J. C. (2011). *Heat generation and transport in the Earth*, (pp. 232–260). Cambridge: Cambridge University Press.
Jaupart, C., Mareschal, J. C., Guillou-Frottier, L., & Davaille, A. (1998). Heat flow and thickness of the lithosphere in the Canadian shield. *Journal of Geophysical Research*, *103*, 15269–15286. https://doi.org/10.1029/98JB01395
Jaupart, C., Mareschal, J. C., & Iarotsky, L. (2016). Radiogenic heat production in the continental crust. *Lithos*, *262*, 398–427. https://doi.org/10.1016/j.lithos.2016.07.017
Jellinek, A. M., & Jackson, M. G. (2015). Connections between the bulk composition, geodynamics and habitability of Earth. *Nature Geoscience*, *8*, 587–593. https://doi.org/10.1038/NGEO2488
Jellinek, A. M., & Lenardic, A. (2009). Effects of spatially varying roof cooling on thermal convection at high Rayleigh number in a fluid with a strongly temperature-dependent viscosity. *Journal of Fluid Mechanics*, *629*, 109–137. https://doi.org/10.1017/S0022112009006260

Jull, M., & Kelemen, P. B. (2001). On the conditions for lower crustal convective instability. *Journal of Geophysical Research*, *106*, 6423–6446. https://doi.org/10.1029/2000JB900357

Korenaga, J. (2008). Urey ratio and the structure and evolution of Earth's mantle. *Reviews of Geophysics*, *46*, 2007RG000241. https://doi.org/10.1029/2007RG000241

Lee, C. T. A., Lenardic, A., Cooper, C. M., Niu, F., & Levander, A. (2005). The role of chemical boundary layers in regulating the thickness of continental and oceanic thermal boundary layers. *Earth and Planetary Science Letters*, *230*, 379–395. https://doi.org/10.1016/j.epsl.2004.11.019

Lenardic, A., Moresi, L., Jellinek, A. M., & Manga, M. (2005). Continental insulation, mantle cooling, and the surface area of oceans and continents. *Earth and Planetary Science Letters*, *234*, 317–333. https://doi.org/10.1016/j.epsl.2005.01.038

Lenardic, A., Moresi, L., Jellinek, A. M., O'Neill, C. J., Cooper, C. M., & Lee, C. T. (2011). Continents, supercontinents, mantle thermal mixing, and mantle thermal isolation: Theory, numerical simulations, and laboratory experiments. *Geochemistry, Geophysics, Geosystems*, *12*, Q10016. https://doi.org/10.1029/2011GC003663

Li, Y., Deschamps, F., & Tackley, P. J. (2014). The stability and structure of primordial reservoirs in the lower mantle: Insights from models of thermochemical convection in three-dimensional spherical geometry. *Geophysical Journal International*, *199*, 914–930. https://doi.org/10.1093/gji/ggu295

Limare, A., Vilella, K., Di Giuseppe, E., Farnetani, C., Kaminski, E., Surducan, E., et al. (2015). Microwave-heating laboratory experiments for planetary mantle convection. *Journal of Fluid Mechanics*, *1565*, 14–18. https://doi.org/10.1017/jfm.2015.347

McKenzie, D., & Bickle, M. J. (1988). The volume and composition of melt enerated by extension of the lithosphere. *Journal of Petrology*, *29*, 625–679. https://doi.org/10.1093/petrology/29.3.625

Mooney, W. D., Laske, G., & Masters, T. G. (1998). CRUST 5.1: A global crustal model at 5° × 5°. *Journal of Geophysical Research*, *103*, 727–747. https://doi.org/10.1029/97JB02122

Moresi, L. N., & Solomatov, V. S. (1995). Numerical investigation of 2D convection with extremely large viscosity variations. *Physics of Fluids*, *7*, 2154–2162. https://doi.org/10.1063/1.868465

Moresi, L. N., & Solomatov, V. (1998). Mantle convection with a brittle lithosphere: Thoughts on the global tectonic styles of the Earth and Venus. *Geophysical Journal International*, *133*, 669–682. https://doi.org/10.1046/j.1365-246X.1998.00521.x

Nakagawa, T., & Tackley, P. J. (2004). Effects of thermo-chemical mantle convection on the thermal evolution of the Earth's core. *Earth and Planetary Science Letters*, *220*, 107–119. https://doi.org/10.1016/S0012-821X(04)00055-X

Parmentier, E. M., & Sotin, C. (2000). Three-dimensional numerical experiments on thermal convection in a very viscous fluid: Implications for the dynamics of a thermal boundary layer at high Rayleigh number. *Physics of Fluids*, *12*, 609–617. https://doi.org/10.1063/1.870267

Pasyanos, M. E., Masters, T. G., Laske, G., & Ma, Z. (2014). LITHO1.0: An updated crust and lithospheric model of the Earth. *Journal of Geophysical Research: Solid Earth*, *119*, 2153–2173. https://doi.org/10.1002/2013JB010626

Putirka, K. D., Perfit, M., Ryerson, F. J., & Jackson, M. G. (2007). Ambient and excess mantle temperatures, olivine thermometry, and active vs. passive upwelling. *Chemical Geology*, *241*, 177–206. https://doi.org/10.1016/j.chemgeo.2007.01.014

Rolf, T., Coltice, N., & Tackley, P. J. (2012). Linking continental drift, plate tectonics and the thermal state of the earth's mantle. *Earth and Planetary Science Letters*, *351*, 134–146.

Rolf, T., & Tackley, P. J. (2011). Focusing of stress by continents in 3D spherical mantle convection with self-consistent plate tectonics. *Geophysical Research Letters*, *38*, L18301. https://doi.org/10.1029/2011GL048677

Sella, G. F., Dixon, T. H., & Mao, A. (2002). REVEL: A model for Recent plate velocities from space geodesy. *Journal of Geophysical Research*, *107*, ETG 11-1–ETG 11-30. https://doi.org/10.1029/2000JB000033

Sharpe, H., & Peltier, W. R. (1978). Parameterized mantle convection and the Earth's thermal history. *Geophysical Research Letters*, *5*, 737–740. https://doi.org/10.1029/GL005i009p00737

Stein, C., Lowman, J. P., & Hansen, U. (2013). The influence of mantle internal heating on lithospheric mobility: Implications for super-Earths. *Earth and Planetary Science Letters*, *361*, 448–459. https://doi.org/10.1016/j.epsl.2012.11.011

Tackley, P. J. (1998). Self-consistent generation of tectonic plates in three-dimensional mantle convection. *Earth and Planetary Science Letters*, *157*, 9–22. https://doi.org/10.1016/S0012-821X(98)00029-6

Tackley, P. J. (2000a). Self-consistent generation of tectonic plates in time-dependent, three-dimensional mantle convection simulations 1. Pseudoplastic yielding. *Geochemistry, Geophysics, Geosystems*, *1*, 2000GC000036. https://doi.org/10.1029/2000GC000036

Tackley, P. J. (2000b). Self-consistent generation of tectonic plates in time-dependent, three-dimensional mantle convection simulations 2. Strain weakening and asthenosphere. *Geochemistry, Geophysics, Geosystems*, *1*, 2000GC000043. https://doi.org/10.1029/2000GC000043

Tackley, P. J. (2008). Modeling compressible mantle convection with large viscosity contrasts in a three-dimensional spherical shell using the yin-yang grid. *Physics of the Earth and Planetary Interiors*, *171*, 7–18. https://doi.org/10.1016/j.pepi.2008.08.005.

Taylor, S. R., & McLennan, S. M. (1995). The geochemical evolution of the continental crust. *Reviews of Geophysics*, *33*, 241–265. https://doi.org/10.1029/95RG00262

Travis, B., Weinstein, S., & Olson, P. (1990). Three-dimensional convection planforms with internal heat generation. *Geophysical Research Letters*, *17*, 243–246. https://doi.org/10.1029/GL017i003p00243

Trompert, R., & Hansen, U. (1998). Mantle convection simulations with rheologies that generate plate-like behavior. *Nature*, *395*, 686–689. https://doi.org/10.1038/27185

Vilella, K. (2020). *Heat-blanketed convection and its implications for the continental lithosphere*. Mendeley Data, Version 3. https://doi.org/10.17632/25pf8kj678.3

Vilella, K., & Deschamps, F. (2018). Temperature and heat flux scaling laws for isoviscous, infinite Prandtl number mixed heating convection. *Geophysical Journal International*, *214*, 265–281. https://doi.org/10.1093/gji/ggy138

Vilella, K., & Kaminski, E. (2017). Fully determined scaling laws for volumetrically heated convective systems, a tool for assessing habitability of exoplanets. *Physics of the Earth and Planetary Interiors*, *266*, 18–28. https://doi.org/10.1016/j.pepi.2017.02.001

Vilella, K., Limare, A., Jaupart, C., Farnetani, C., Fourel, L., & Kaminski, E. (2018). Fundamentals of laminar free convection in internally heated fluids at values of the Rayleigh-Roberts number up to 10^9. *Journal of Fluid Mechanics*, *846*, 966–998. https://doi.org/10.1017/jfm.2018.316

White, D. B. (1988). The planforms and onset of convection with a temperature-dependent viscosity. *Journal of Fluid Mechanics*, *191*, 247–286. https://doi.org/10.1017/S0022112088001582

Whitehead, J. A., & Behn, M. D. (2015). The continental drift convection cell. *Geophysical Research Letters*, *42*, 4301–4308. https://doi.org/10.1002/2015GL064480

Whitehead, J. A., Jr, & Parsons, B. (1977). Observations of convection at Rayleigh numbers up to 760,000 in a fluid with large Prandtl number. *Geophysical & Astrophysical Fluid Dynamics*, *9*, 201–217. https://doi.org/10.1080/03091927708242327

Yoshida, M. (2013). Mantle temperature under drifting deformable continents during the supercontinent cycle. *Geophysical Research Letters*, *40*, 681–686. https://doi.org/10.1002/grl.50151

Zhong, S., & Gurnis, M. (1993). Dynamic feedback between a continent like raft and thermal convection. *Journal of Geophysical Research*, *98*, 12219–12232. https://doi.org/10.1029/93JB00193

Zhong, S., & Gurnis, M. (1995). Mantle convection with plates and mobile, faulted plate margins. *Science*, *267*, 838–843. https://doi.org/10.1126/science.267.5199.838